

- (14) G. Silvestri, S. Gambino, M. Guainazzi, and R. Ercoli, *J. Chem. Soc., Dalton Trans.*, 2558 (1972).  
 (15) N. A. Beach and H. B. Gray, *J. Am. Chem. Soc.*, **90**, 5713–5721 (1968).  
 (16) R. Orbach, *Proc. Phys. Soc., London*, **77**, 821–826 (1961).  
 (17) N. J. Hill, *J. Chem. Soc., Faraday Trans. 2*, **68**, 427–434 (1972).  
 (18) I. A. Miller and E. L. Offenbacher, *Phys. Rev.*, **166**, 269–278 (1968).  
 (19) B. Bleaney and M. C. M. O'Brien, *Proc. Phys. Soc., London, Sect. B*, **29**, 1216–1229 (1956).  
 (20) K. W. H. Stevens, *Proc. R. Soc., London, Part A*, **219**, 542–555 (1953).  
 (21) M. Gerloch and J. S. Miller, *Prog. Inorg. Chem.*, **10**, 17 (1968).  
 (22) H. Kamimura, *J. Phys. Soc. Jpn.*, **11**, 1171–1181 (1956).  
 (23) T. M. Dunn, *Trans. Faraday Soc.*, **57**, 1441–1444 (1961).  
 (24) R. M. Golding, "Applied Wave Mechanics", Van Nostrand, London, 1969, Chapter 7.  
 (25) K. H. Hausser, *Z. Naturforsch. A*, **16**, 1190–1192 (1961).  
 (26) G. Henrici-Olive, S. Olive, *Z. Phys. Chem. (Frankfurt am Main)*, **56**, 223–231 (1967).  
 (27) E. Konig, *Z. Naturforsch. A*, **19**, 1139–1147 (1964).  
 (28) B. R. McGarvey, *J. Phys. Chem.*, **71**, 51–67 (1967).  
 (29) W. T. Oosterhuis and G. Lang, *Phys. Rev.*, **138**, 439–456 (1969).

## The Heat Capacity, Conductivity, and Crystal Structure of Tetrathiafulvalenium 2,5-Diethyltetracyanoquinodimethane

Arthur J. Schultz,<sup>1a</sup> Galen D. Stucky,\*<sup>1a</sup> Robert Craven,<sup>1b</sup>  
 Mark J. Schaffman,<sup>1b</sup> and Myron B. Salamon<sup>1b</sup>

*Contribution from the Department of Chemistry and Materials Research Laboratory, University of Illinois, Urbana, Illinois 61801, and the Department of Physics and Materials Research Laboratory, University of Illinois, Urbana, Illinois 61801.*

*Received August 11, 1975*

**Abstract:** The single-crystal room temperature structure and measurements of the conductivity and heat capacity in the vicinity of the metal insulator transition have been determined for the pseudo-one-dimensional charge transfer salt tetrathiafulvalenium 2,5-diethyltetracyanoquinodimethane (TTF-DETCNQ). The compound crystallizes in space group  $P\bar{1}$  with cell dimensions  $a = 13.654$  (4) Å,  $b = 3.859$  (1) Å,  $c = 10.094$  (3) Å,  $\alpha = 97.00$  (2)°,  $\beta = 96.25$  (2)°, and  $\gamma = 85.91$  (2)°. The perpendicular interplanar distances along the segregated stacks are 3.598 (1) Å for TTF and 3.257 (1) Å for DETCNQ. The metal insulator transition observed in the conductivity measurements in the  $b$ -axis direction is sharply defined by a peak in the heat capacity curve at 111 K. Assuming a single band model, we estimate the density of states at the Fermi surface to be  $5.7 \text{ eV}^{-1}$ . The effect on the transition temperature of changes in the density of states, degree of charge transfer, and stacking distances are discussed.

One of the methods used in trying to understand the metal insulator transition in the highly conducting charge transfer salt TTF-TCNQ<sup>2</sup> has been the study of chemically modified TTF-TCNQ compounds. The goal of these investigations has been to synthesize new materials with minimal structural changes so that the effects of crystal disorder,<sup>3–5</sup> intra- and interchain coupling,<sup>6</sup> ionization potential, and polarizability on the metal insulator transition and the high temperature conductivity of a series of crystals can be studied.

The TTF-TTF interplanar distances in the one-dimensional systems which have been investigated are 3.47 Å<sup>7</sup> or greater. This spacing is comparable to van der Waals distances associated with nonbonded interactions between organic groups, and it is not surprising that numerous derivatives of TTF<sup>8–11</sup> or TSF<sup>12–15</sup> (the selenium analogue of TTF) are known to form highly conducting complexes with TCNQ. The TCNQ-TCNQ interplanar spacing in TTF-TCNQ is 3.16 Å.<sup>7</sup> This is well below the van der Waals contact for even aromatic carbon atoms (~3.34 Å) so that it can be expected that it will be much more difficult to obtain a closely stacked lattice and metallic behavior with substituted TCNQ. In fact, metallic behavior has not been previously reported for any derivatives of TCNQ, other than the very distantly related TNAP,<sup>16</sup> the 2,6-tetracyanoquinodimethane derivative of naphthalene.

In this paper, we present the details of the room temperature structure and the specific heat and electrical conductivity in the vicinity of the metal insulator transition of the substituted TCNQ charge transfer salt tetrathiafulvalenium 2,5-diethyltetracyanoquinodimethane (TTF-DETCNQ). A preliminary screening of this and other substituted TCNQ complexes with TTF by Groff<sup>17</sup> of Du Pont Laboratories suggested

that a number of these materials are metallic. The fact that one can substitute organic groups on the TCNQ molecule and maintain cooperative behavior greatly expands the potential number of one-dimensional metallic systems which can be made. It also suggests the feasibility of forming conducting materials with TCNQ molecules attached to an organic polymeric backbone or forming donor-acceptor pairs joined together through chemical bonds. Further investigation of the low temperature crystal and molecular structure of TTF-DETCNQ is currently underway and will be reported in a subsequent publication.

### Experimental Section

**Collection and Reduction of the X-Ray Data.** The crystals used in this study were prepared by Drs. R. C. Wheland and E. L. Martin of the Du Pont Central Research Department<sup>18</sup> and graciously supplied to us by Dr. L. J. Guggenberger. The long, black colored crystals appear as bundles of square, cross-sectioned fibers, rather than stacks of thin plates, as in TTF-TCNQ. Weissenberg and precession photographs revealed no systematic extinctions or other indications of symmetry. Therefore, a primitive cell for the triclinic space group  $P\bar{1}$  was chosen with the  $b$  axis parallel to the needle axis of the crystal. The cell dimensions were refined from the angular diffractometer settings of 20 centered reflections and are  $a = 13.654$  (4) Å,  $b = 3.859$  (1) Å,  $c = 10.094$  (3) Å,  $\alpha = 97.00$  (2)°,  $\beta = 96.25$  (2)°,  $\gamma = 85.91$  (2)°, and  $V = 523.8$  Å<sup>3</sup>. The assumption of the centrosymmetric space group  $P\bar{1}$  is justified by the satisfactory agreement ultimately obtained. With one formula weight of TTF-DETCNQ per unit cell, the calculated density is  $1.473 \text{ g/cm}^3$ .

Numerous crystals were examined on the diffractometer and found to be twinned or have very large mosaicities. The crystal finally selected for intensity measurements was mounted in a thin-walled glass

Table I. Final Parameters for TTF-DETCNQ

Atom	$x^a$	$y$	$z$	$B$ ( $\text{\AA}^2$ ) <sup>b</sup>
S(1)	-0.132 56 (5)	-0.0962 (2)	0.088 28 (7)	<i>c</i>
S(2)	0.076 16 (5)	-0.1191 (2)	0.192 21 (7)	<i>c</i>
N(1)	0.333 9 (2)	-0.5125 (6)	0.839 9 (2)	<i>c</i>
N(2)	0.192 0 (2)	-0.4810 (7)	0.461 6 (2)	<i>c</i>
C(1)	-0.102 6 (2)	-0.1811 (9)	0.250 6 (3)	<i>c</i>
C(2)	-0.008 8 (2)	-0.1927 (9)	0.297 4 (3)	<i>c</i>
C(3)	-0.011 8 (2)	-0.0449 (7)	0.059 3 (2)	<i>c</i>
C(4)	0.347 0 (2)	-0.4173 (7)	0.740 8 (3)	<i>c</i>
C(5)	0.263 7 (2)	-0.4052 (7)	0.524 8 (2)	<i>c</i>
C(6)	0.351 6 (2)	-0.3180 (6)	0.609 4 (2)	<i>c</i>
C(7)	0.427 7 (2)	-0.1586 (6)	0.561 7 (2)	<i>c</i>
C(8)	0.414 1 (2)	-0.0827 (6)	0.424 5 (2)	<i>c</i>
C(9)	0.519 7 (2)	-0.0675 (6)	0.638 1 (2)	<i>c</i>
C(10)	0.541 7 (2)	-0.1366 (7)	0.783 2 (2)	<i>c</i>
C(11)	0.646 7 (2)	-0.0763 (8)	0.846 7 (3)	<i>c</i>
H(1)	-0.150 (2)	-0.207 (6)	0.307 (2)	3.0 <sup>d</sup>
H(2)	0.020 (2)	-0.245 (6)	0.374 (2)	3.0
H(8)	0.353 (2)	-0.133 (6)	0.379 (2)	3.0
H(10A)	0.493 (2)	0.007 (6)	0.837 (2)	3.0
H(10B)	0.529 (2)	-0.393 (6)	0.787 (2)	3.0
H(11A)	0.693 (2)	-0.214 (6)	0.792 (2)	3.0
H(11B)	0.652 (2)	-0.138 (6)	0.938 (2)	3.0
H(11C)	0.661 (2)	0.174 (7)	0.854 (2)	3.0

Anisotropic Thermal Parameters ( $\times 10^3$ ) <sup>e</sup>						
Atom	$\beta_{11}$	$\beta_{22}$	$\beta_{33}$	$\beta_{12}$	$\beta_{13}$	$\beta_{23}$
S(1)	3.25 (4)	99.2 (9)	11.0 (1)	-2.2 (1)	0.60 (5)	2.1 (2)
S(2)	3.79 (4)	100.6 (8)	9.83 (9)	-0.9 (1)	-0.44 (5)	2.1 (2)
N(1)	5.4 (2)	96 (2)	8.2 (3)	-1.9 (5)	1.8 (2)	10.1 (7)
N(2)	4.5 (2)	122 (3)	11.6 (3)	-6.8 (5)	-0.7 (2)	7.5 (8)
C(1)	5.3 (2)	103 (3)	11.7 (4)	-2.9 (7)	2.7 (2)	4.6 (9)
C(2)	6.0 (2)	107 (3)	10.0 (4)	-1.0 (7)	0.1 (2)	8.1 (9)
C(3)	3.3 (1)	67 (2)	8.9 (3)	-0.1 (5)	0.0 (2)	-1.0 (7)
C(4)	3.1 (1)	51 (2)	8.0 (3)	-1.9 (4)	1.0 (2)	2.4 (7)
C(5)	4.1 (2)	62 (2)	7.2 (3)	-1.7 (5)	1.2 (2)	7.7 (7)
C(6)	3.2 (1)	51 (2)	5.5 (3)	-0.9 (4)	0.5 (2)	3.7 (6)
C(7)	3.3 (1)	38 (2)	5.1 (3)	-0.4 (4)	0.7 (1)	2.0 (6)
C(8)	3.0 (1)	43 (2)	5.8 (3)	-1.3 (4)	-0.1 (2)	1.9 (6)
C(9)	3.3 (1)	36 (2)	4.9 (2)	-0.1 (4)	0.5 (1)	1.6 (5)
C(10)	4.1 (2)	48 (2)	5.3 (3)	-1.4 (5)	0.1 (2)	4.4 (6)
C(11)	5.1 (2)	69 (3)	6.1 (3)	-4.2 (6)	-0.9 (2)	6.4 (7)

<sup>a</sup> $x, y, z$  are fractional coordinates. <sup>b</sup>Isotropic temperature factor of the form  $\exp(-B^2 \sin^2 \theta / \lambda)$ . <sup>c</sup>Atoms refined anisotropically.

<sup>d</sup>Hydrogen temperature factors were not refined. <sup>e</sup>Anisotropic temperature factors of the form  $\exp\{-(h^2\beta_{11} + k^2\beta_{22} + l^2\beta_{33} + 2hk\beta_{12} + 2hl\beta_{13} + 2kl\beta_{23})\}$ .

capillary and had approximate dimensions of  $0.14 \times 0.54 \times 0.22 \text{ mm}^3$ . It showed some evidence of twinning in the  $a^*$  direction, but its average mosaic spread as determined from narrow source-open counter  $\omega$  scans of several reflections was a reasonable  $0.21 \pm 0.03^\circ$ . The intensity data were collected by the  $\theta$ - $2\theta$  scan technique on a Picker FACS-I diffractometer using Mo  $K\alpha$  radiation with a graphite monochromator. Reflections were measured with calculated  $2\theta$  values between 5 and  $50^\circ$  at a scan rate of  $2^\circ/\text{min}$  and with background counts of 10 s at each end of the scan. A symmetrical scan range of  $1.8^\circ$  in  $2\theta$  was used with allowance made for  $K\alpha_1$ - $K\alpha_2$  separation.

The intensities of 1898 independent reflections were measured and corrected for Lorentz and polarization effects to yield a net of  $|F_o|$  values where  $F_o$  is the observed structure factor amplitude. This led to 1261 reflections having  $F_o^2 \geq 3\sigma(F_o^2)$ . The standard deviations  $\sigma(F_o^2)$  were estimated according to the formula

$$\sigma(F_o^2) = (Lp)^{-1}[S + (B_1 + B_2)(T_s/2T_B)^2 + (0.02I)^2]^{1/2}$$

where  $S$  and  $B_1$  and  $B_2$  are the scan and background counts in times  $T_s$  and  $T_B$ ,  $Lp$  is the Lorentz-polarization factor, and  $I$  is the integrated intensity. The data were not corrected for absorption ( $\mu = 4.58 \text{ cm}^{-1}$ ). Errors due to this neglect are estimated to be less than 1% of the measured intensities.

**Solution and Refinement of the Structure.** The 253 normalized structure factors with  $|E| \geq 1.50$  as calculated by FAME<sup>19</sup> were used in the MULTAN<sup>20</sup> program package to solve the structure by direct methods. The Fourier calculations based on the three sets of phases all having the highest figure of merit<sup>20</sup> did not reveal any structural

fragments that made chemical sense. Finally, an  $E$ -map calculated from a set of phased  $|E|$ 's with the second highest figure of merit yielded the two sulfur and three carbon atoms of the TTF molecule situated on the inversion center at  $(0,0,1/2)$ . Refinement of the positional parameters using data with  $F_o^2 \geq 3\sigma(F_o^2)$  led to a weighted agreement factor  $R_w = (\sum w(|F_o| - |F_d|)^2 / \sum w |F_o|^2)^{1/2}$  of 0.518. The function minimized in the least-squares refinements was  $\sum w(|F_o| - |F_d|)^2$  where the weights  $w$  were assigned as  $2F_o/\sigma(F_o^2)$ . All the nonhydrogen atoms in the DETCNQ molecule were located by a sequence of least-squares refinements and difference Fourier syntheses. The neutral atomic scattering factors used in these refinements for the nonhydrogen atoms were those of Cromer and Waber.<sup>21</sup> The sulfur atoms were treated for anomalous dispersion using the values of  $\Delta f'$  and  $\Delta f''$  tabulated by Cromer.<sup>22</sup>

For esthetic reasons, the origin was shifted such that the TTF was situated on the inversion center at  $(0,0,0)$  and the DETCNQ was situated on the inversion center at  $(1/2,0,1/2)$ . Refinement of all the atoms with anisotropic thermal parameters and using all of the data (including  $F_o = 0$ ) led to agreement factors  $R (= \sum |F_o| - |F_c| / \sum |F_o|)$  and  $R_w$  of 0.111 and 0.085, respectively. A difference Fourier revealed the positions of all eight independent hydrogen atoms. Surprisingly, the peaks on the Fourier map of the five ethyl hydrogen atoms were all higher than those for the ring hydrogen atoms, indicating minimal disorder in the ethyl substituent. Hydrogen atom scattering factors from Stewart et al.<sup>23</sup> were used in refining the positional parameters of the hydrogen atoms. The parameters for all the atoms obtained from the final refinement with  $R = 0.070$  and  $R_w = 0.039$  are presented in Table I. The final standard deviation of an observation of unit weight was 1.52 and the highest peak on the final difference Fourier was  $0.407 \text{ e}/\text{\AA}^3$ , or about 57% of the average hydrogen atom in this structure. A tabulation of the 1898 observed and calculated structure factor amplitudes used in the final refinement is available.<sup>24</sup>

**Heat Capacity Measurements.** Heat capacity measurements were made on single crystals of this material using ac calorimetry.<sup>25-27</sup> This technique, which has been used successfully to characterize the thermal properties of TTF-TCNQ in the vicinity of its metal insulator transition,<sup>28,29</sup> has very high sensitivity and can be used with very small ( $\sim 10 \mu\text{g}$ ) samples.

Crystals, which were chosen on the basis of size and uniformity, were mounted (as shown in Figure 1) on a pair of thermocouples using silicon vacuum grease or GE7031 cement. This thermocouple pair is formed by first spot welding lengths  $25 \mu\text{m}$  thick and  $\approx 0.5 \text{ mm}$  in width.

The sample-thermocouple combination was heated by chopped pulses of light from a quartz-iodide lamp which was driven by a regulated dc current supply. One of the junctions of the crossed thermocouples detected the temperature oscillations of the sample with respect to the adjacent copper heat sink, while the other formed the cold junction of a chromel-alumel thermocouple with its hot junction at the ice point. The time averaged sample temperature was measured with this hot-cold thermocouple pair and a potentiometer. The magnitude of the thermal oscillations of the thermocouple-sample combination was measured with a lock-in amplifier phase locked directly to the chopper frequency. The magnitude of the temperature oscillations and the temperature of the sample were continuously recorded.

The dynamic temperature excursions of the sample in this configuration can be described in terms of two time constants:  $\tau_1$ , which characterizes the thermal coupling between the sample and its surroundings, and  $\tau_2$ , the time for the sample to reach internal thermal equilibrium. In the present experiment, the major thermal coupling between the sample and the copper heat sink is provided by a helium exchange gas. When the angular frequency of the chopped light is such that  $\omega\tau_2 \ll 1$ , i.e., when the sample comes to equilibrium with itself much faster than that chopping period, the sample temperature satisfies an equation

$$C(T) \frac{dT}{dt} + kT = \frac{1}{2} P_0 [1 + s(t)]$$

where  $C(T)$  is the heat capacity of the sample,  $k$  the thermal conductance of the gas (assumed to be constant),  $P_0$  is the power absorbed by the sample while the light is on it, and  $s(t)$  is a square wave of unit amplitude and period  $2\pi/\omega$ . The steady state solution,  $\omega\tau_1 > 1$  gives an average temperature rise of the sample of  $P_0/2k$  over the copper

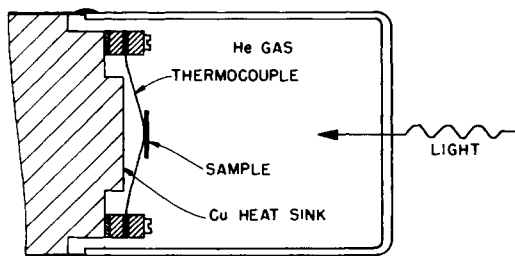


**Figure 1.** Experimental arrangement for specific heat measurements. The light comes from tungsten-iodide lamp, chopped by a mechanical chopper. The primary heat flow is along a line from right to left.

heat sink with an oscillatory part  $CdT_{ac}/dT = P_0\delta(t)/2$ . For small oscillations,  $C(T)$  is approximately constant and the above equation can be integrated to give a triangular wave form of amplitude  $|T_{ad}| = P_0/2\pi\omega C$ . The inverse of the temperature oscillations is directly proportional to the heat capacity of the sample.

Although the exact time constants are not known a priori, the correct operating range can be found by measuring the amplitude of the triangular temperature oscillations as a function of the chopping frequency with a broad band amplifier. The operating frequency, in this case 9 Hz, is chosen to be well within the region where  $|T_{ad}| \propto 1/\omega$ . Using known thermal conductivities of the gas and simultaneous measurement of the temperature offset,  $P_0/2k$ , and the temperature oscillations, it is possible to get an absolute measurement of the specific heat, but experimental limitations of low frequency preamplifier roll-off and small dc voltage measurements limit the accuracy of this number. We have chosen instead to calibrate the specific heat relative to dc measurements made on bulk samples of TTF-TCNQ. We expect that due to the structural similarity of these two systems the large lattice background will be within the 10% accuracy of the absolute measurements. Our relative accuracy is much higher, however, and allows us to characterize the thermal behavior of TTF-DETCNQ in the vicinity of its metal insulator phase transition.

The specific heat of one sample of TTF-DETCNQ in the vicinity of its metal insulator phase transition is shown in Figure 2. This sample weighed 85  $\mu\text{g}$  and was  $\approx 2.5$  mm long by 0.25 mm in length. The total lattice specific heat in this region is quite large,  $\approx 24R$  ( $R = 8.317 \text{ J K}^{-1} \text{ mol}^{-1}$ ), due to the large number of atoms per unit cell and contributions from low frequency optical phonon branches.<sup>30</sup> The major feature of this specific heat data is the anomaly at 111 K. This anomaly occurs at the same temperature as the sharp change in the electrical conductivity and we associate it with a two- or three-dimensional ordering within the crystal which drives the metal insulator transition. No other anomalies were observed between 15 and 300 K.

In order to examine the transition of this sample more closely, we have subtracted a smooth lattice background, fit to the data above the transition temperature. The resulting data, along with that from another crystal of TTF-DETCNQ, which was 112  $\mu\text{g}$ , are shown in Figure 3. The height of the specific heat anomaly is  $2R$  to  $3.5R$ . The entropy associated with the transition, obtained from direct numerical integration of only the data in this figure is  $0.64R$  and  $0.085R$  for the high peak and low peak, respectively. This does not include the contribution to the total entropy of the transition from temperatures below 99 K. Either a linear model for the specific heat in this region or a BCS-like formulation gives about  $0.1R$  of entropy for this region if they are normalized to the 99 K data.

**Electrical Conductivity Measurements.** Electrical conductivity measurements were made on single crystals of TTF-DETCNQ using a standard four probe dc measurement technique. The samples were mounted with Du Pont conductive silver composition no. 7941 on four  $25 \mu\text{m Au}_{0.9}\text{Cu}_{0.1}$  annealed alloy wires with care taken to surround the samples with the silver paint at the contacts to minimize the possibility of spurious current paths. The wires were loosely suspended on a mylar form in order to reduce the strain of the contacts upon cooling, but despite this precaution many samples cracked and became electrically discontinuous between room temperature and 200 K. Temperature measurement was made with a cromel-alumel thermocouple junction with the cold point being adjacent to the sample being measured and in thermal contact through an atmosphere of helium gas. Up to four samples were run at one time, each having its own thermometer. Data were taken by successively switching the constant measurement current from one sample to another and re-

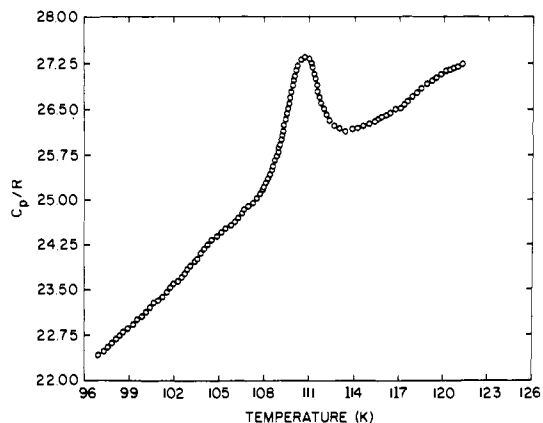


**Figure 2.** The specific heat in the vicinity of the metal insulator phase transition.

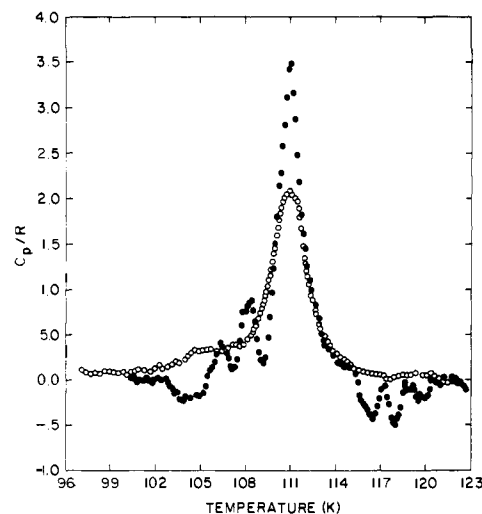


**Figure 3.** The specific heat of two samples minus the lattice specific heat background.

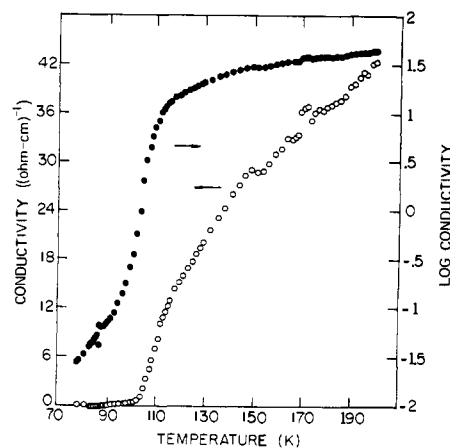


**Figure 4.** The conductivity and log of the conductivity of one sample. The point of maximum slope in the plot of the conductivity vs. temperature is at the phase transition.

coding the voltage through an analog to digital converter onto paper tape. Typical measurement currents were  $\leq 1 \text{ mA}$  or  $\leq 1 \text{ A/cm}^2$ .

Above the metal insulator phase transition, there was no evidence that the sample was being driven out of thermal equilibrium with the thermocouple junction by joule heating. The possible error in the absolute temperature displayed in this data and in the specific heat data is about  $\pm 1 \text{ K}$ . All thermocouple junctions were not separately calibrated against a standard resistance thermometer, but those which were showed variance of this magnitude.

The results for one of the samples are displayed in Figure 4. This sample was  $0.038 \times 0.025 \text{ cm}$  in cross section with the voltage contacts

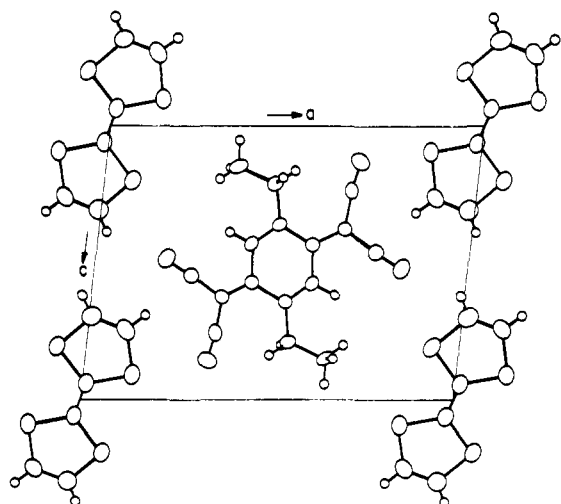


Figure 5. The crystal packing of TTF-DETCNQ as viewed parallel to the *b* axis.

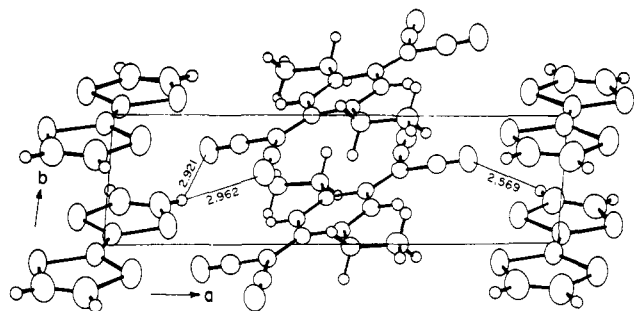


Figure 6. The crystal packing of TTF-DETCNQ as viewed approximately perpendicular to the *ab* plane.

0.109 (5) cm apart. Both the conductivity and the logarithm of the conductivity are presented to allow comparison with the conductivities of TTF-TCNQ and to emphasize the region near the metal insulator phase transition. The shape of these data are typical for samples which survived cooling to 77 K. Above 200 K, the data are much noisier. It is possible that this is due to poor contacts since topographically bizarre current paths become more possible and more misleading<sup>31</sup> as the conductivity along the *b* axis of the crystal and the subsequent anisotropy become greater. This high temperature noise has also been seen in some preliminary measurements by workers at the Du Pont laboratories.<sup>17</sup> The samples become too resistive for our measuring technique below 50 K, but no other anomalies were seen to this temperature.

### Description of the Structure

The crystal packing of the TTF-DETCNQ molecules is shown in Figures 5 and 6. Analogous to TTF-TCNQ,<sup>7</sup> there are separate chains of TTF and DETCNQ stacking parallel to the *b* axis. However, whereas in TTF-TCNQ the donors and acceptors each form a herringbone pattern in the *bc* plane, in TTF-DETCNQ all the TTF molecules and all the DETCNQ molecules are crystallographically required to have the same orientations. This same type of packing is seen in crystals of TTF-TNAP.<sup>16</sup> Furthermore, the angle between the TTF and DETCNQ molecular planes (Table IV) is only 19.8°, as compared to 58.5° in TTF-TCNQ between nearest neighbors. The closest intermolecular contacts are those between N(2)⋯H(2), N(2)⋯H(1) and N(1)⋯H(1) at values of 2.57, 2.92, and 2.96 Å, respectively. With the cyano groups of the DETCNQ molecule pointing inbetween the TTF molecules along the stack, the pairs of short nitrogen-sulfur contacts are 3.413 and 3.563 Å for N(1)⋯S(1) and 3.394 and 3.734 Å for N(2)⋯S(2). There are no contacts between the ethyl hydrogens and the TTF molecules of less than 3.0 Å. In addition, there

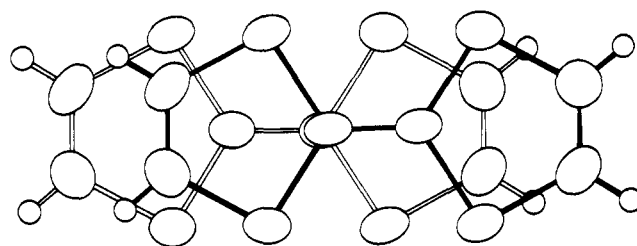


Figure 7. Projection of the overlap between neighboring TTF molecules viewed perpendicular to the molecular planes.

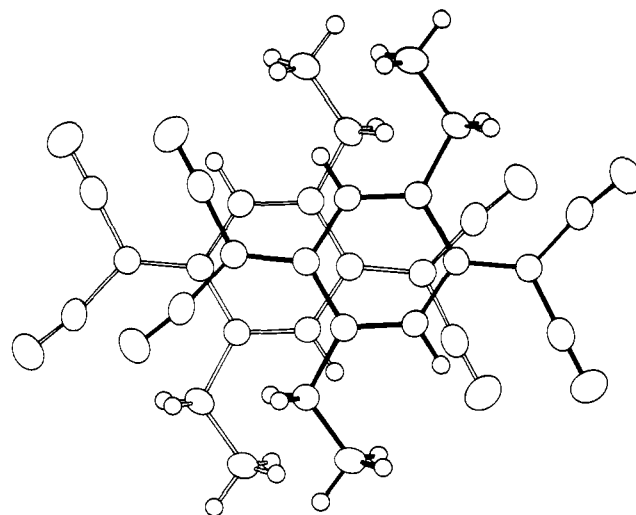


Figure 8. Projection of the overlap between neighboring DETCNQ molecules viewed perpendicular to the molecular planes.

is no evidence (*vide ante*) for a superlattice based on long range ordering of the ethyl groups.

The angles between the *b* axis and the normals to the molecular planes are 21.2 and 32.4° for TTF and DETCNQ, respectively. The perpendicular interplanar distances are 3.598 (1) Å for TTF and 3.257 (1) Å for DETCNQ. These are significantly longer than the corresponding values of 3.473 (2) and 3.168 (2) Å in TTF-TCNQ, but the TCNQ-TCNQ distance of 3.26 (1) Å in NMP-TCNQ (*N*-methylphenazinium tetracyanoquinodimethane)<sup>32</sup> is the same as that for DETCNQ in this structure. Projections perpendicular to the molecular planes along the stacks are shown in Figures 7 and 8. The TTF-TTF overlap appears to be identical with that in TTF-TCNQ, while the overlap of the DETCNQ molecules is slightly less symmetric than that for the unsubstituted TCNQ due to the steric requirements of the ethyl groups. It is also apparent from Figure 8 that tris- or tetrasubstitution would make close TCNQ stacking sterically unfeasible, and that disubstitution in ortho positions could only be effective if every other TCNQ molecule along the stack was "flipped over".

The principal intermolecular bond angles and distances are given in Table II using the labeling scheme shown in Figures 9 and 10. Each molecule is situated on a crystallographic center of inversion. In addition, if *mmm* symmetry is assumed for TTF, the related bond angles and distances agree to within one standard deviation. The bond angles in the TCNQ moiety are significantly distorted from *mmm* symmetry as shown in Figure 10. This is apparently a result of steric interaction between the ethyl group and the nearest cyano group with non-bonding contacts between C(4) and the methylene hydrogen atoms of 2.49 and 2.70 Å. As shown in Table IV, C(10) is only 0.019 (3) Å from the least-squares plane of the TCNQ moiety, while C(11) is 0.237 (3) Å out of the plane.

Since the bond distances are in good agreement in the

Table II. Principal Intramolecular Distances and Angles for TTF-DETCNQ

Atoms	Distance, Å		Atoms	Angle, deg
	Obsd	Cor-rected <sup>a</sup>		
S(1)-C(1)	1.711 (3)	1.707	S(1)-C(3)-C(3)'	122.2 (3)
S(2)-C(2)	1.716 (3)	1.733	S(2)-C(3)-C(3)'	122.9 (3)
C(1)-C(3)	1.735 (3)	1.754	S(1)-C(3)-S(2)	114.9 (1)
S(2)-C(3)	1.737 (3)	1.745	C(1)-S(1)-C(3)	94.5 (1)
C(1)-C(2)	1.315 (4)	1.322	C(2)-S(2)-C(3)	94.3 (1)
C(3)-C(3)'	1.363 (5)	1.367	C(1)-C(2)-S(2)	118.0 (2)
C(1)-H(1)	0.89 (2)		C(2)-C(1)-S(1)	118.1 (2)
C(2)-H(2)	0.86 (2)		N(1)-C(4)-C(6)	172.5 (3)
N(1)-C(4)	1.143 (3)	1.141	N(2)-C(5)-C(6)	177.0 (4)
N(2)-C(5)	1.145 (3)	1.150	C(4)-C(6)-C(5)	110.3 (2)
C(4)-C(6)	1.434 (3)	1.431	C(4)-C(6)-C(7)	128.4 (2)
C(5)-C(6)	1.431 (3)	1.437	C(5)-C(6)-C(7)	121.3 (2)
C(6)-C(7)	1.400 (3)	1.404	C(6)-C(7)-C(8)	117.7 (2)
C(7)-C(8)	1.440 (3)	1.438	C(6)-C(7)-C(9)	125.5 (2)
C(7)-C(9)	1.443 (3)	1.450	C(8)-C(7)-C(9)	116.9 (2)
C(8)-C(9)'	1.357 (3)	1.359	C(7)-C(8)-C(9)'	125.4 (2)
C(9)-C(10)	1.515 (3)	1.513	C(7)-C(9)-C(8)'	117.7 (2)
C(10)-C(11)	1.527 (4)	1.536	C(7)-C(9)-C(10)	121.2 (2)
C(8)-H(8)	0.95 (2)		C(8)'-C(9)-C(10)	121.0 (2)
C(10)-H(10A)	1.00 (2)		C(9)-C(10)-C(11)	121.0 (2)
C(10)-H(10B)	1.02 (2)			
C(11)-H(11A)	0.97 (2)			
C(11)-H(11B)	0.97 (2)			
C(11)-H(11C)	0.99 (2)			

<sup>a</sup> Corrected for rigid-body motion. The standard deviations are the same as for the observed distances.

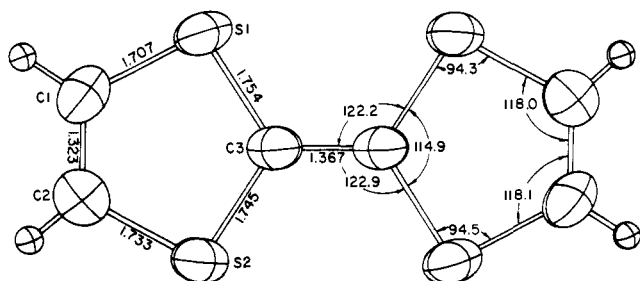


Figure 9. A perspective drawing of the TTF cation.

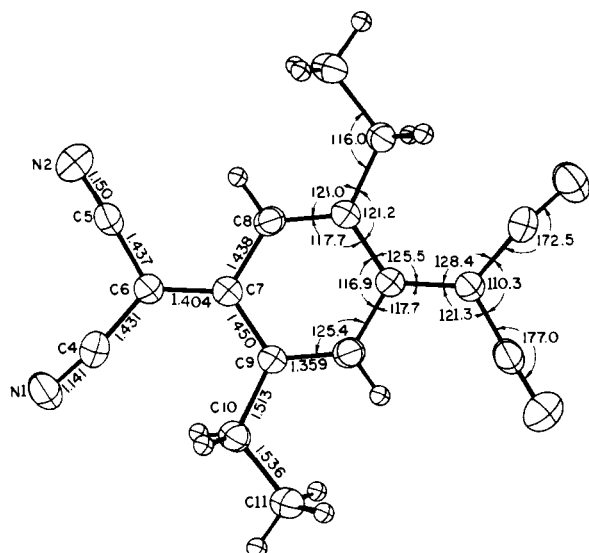


Figure 10. A perspective drawing of the DETCNQ anion.

TCNQ moiety if *mmm* symmetry is assumed, we have tabulated the average values for both TTF and DETCNQ as shown in Table V. In general, it is seen that the bond distances in TTF-DETCNQ lie very close to those in TTF-TCNQ, or fall

Table III. Rigid-Body Thermal Parameters for TTF-DETCNQ

(a) TTF

Tensor Elements $\times 10^4$						
	11	12	13	22	23	33
L (rad <sup>2</sup> )	86 (13)	3 (3)	4 (5)	30 (3)	1 (3)	30 (3)
T (Å <sup>2</sup> )	503 (12)	-32 (11)	-57 (13)	260 (17)	7 (17)	444 (27)

	RMS amplitudes	Principal Axes Direction cosines $\times 10^4$		
		l	m	n
L tensor	5.3° 3.2° 3.1°	9956 807 771	508 -8903 4526	784 -4482 -8905
T tensor	0.23 Å 0.20 Å 0.16 Å	-8522 -5072 -1280	1089 674 -9918	5117 -8592 -22

(b) DETCNQ

Tensor Elements $\times 10^4$						
	11	12	13	22	23	33
L (rad <sup>2</sup> )	31 (3)	-7 (1)	-3 (2)	20 (2)	1 (1)	10 (1)
T (Å <sup>2</sup> )	294 (12)	20 (12)	-20 (13)	261 (15)	-3 (16)	206 (21)

	RMS amplitudes	Principal Axes Direction cosines $\times 10^4$		
		l	m	n
L tensor	3.4° 2.1° 1.8°	8841 4482 1321	-4491 8932 -246	-1290 -376 9909
T tensor	0.18 Å 0.16 Å 0.14 Å	-8981 -3821 -2179	-3957 9181 208	1921 -1050 -9757

between TTF-TCNQ and the corresponding neutral molecule. The latter is the case for all of the bonds in the TTF molecule, which, due to its smaller size, should exhibit the effects of charge to a greater extent than the larger DETCNQ molecule. These results indicate that the charge transfer in TTF-DETCNQ is less than that in TTF-TCNQ.

The rigid-body thermal parameters given in Table III were calculated by the method of Schomaker and Trueblood.<sup>33</sup> The largest librational and translational amplitudes are associated with the axes with the smallest moment of inertia and are labeled *l* for each molecule. In compounds containing unsubstituted TCNQ, *l* is parallel to the C(7)-C(7)' vector, while in DETCNQ the orientation is slightly different due to the presence of the ethyl groups in the 2,5 positions.

## Discussion

When the results of these experiments are analyzed on the basis of a simple model of a Peierls transition, and added to the information about TTF-TCNQ and some of its derivatives, an intriguing picture of the temperature dependence of the phase transitions evolves.

First of all, it is interesting to compare the specific heat information on TTF-DETCNQ with the theory of a Peierls-Frohlich transition developed by Allender, Bray, and Bardeen<sup>34</sup> (ABB) and others.<sup>28,29,35</sup> The total entropy change associated with the metal insulator transition, which consists of the entropy under the peak as given by numerical integration plus that estimated below 99 K, gives an estimate of the density of

Table IV. Least-Squares Planes and the Distances (Å) of the Atoms from Their Respective Planes

In each of the equations of the plane  $X$ ,  $Y$ , and  $Z$  are coordinated ( $R$ ) referred to the orthogonal axis  $a$ ,  $b \times c^*$ , and  $c^*$ . The plane equations have the form  $AX + BY + CZ = D$

The coefficients given below are  $\times 10^4$ .

- (a) TTF molecular plane (non-hydrogen atoms)  
 (b) TTF central plane defined by S(1), C(3), S(2) and their centrosymmetric mates  
 (c) TCNQ plane without ethyl groups (non-hydrogen atoms)  
 (d) TCNQ quinoid ring defined by C(6), C(7), C(8), C(9), and their centrosymmetric mates

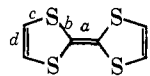
	a	b	c	d
$A$	567	646	3908	3832
$B$	-9388	-9317	-8742	-8752
$C$	-3398	-3575	-2880	-2952
$D$	0	0	15228	14402
S(1)	0.0347 (8)	0.0004 (8)	N(1)	0.004 (2)
S(2)	-0.021 (3)	0.0004 (8)	N(2)	0.011 (3)
C(1)	-0.021 (3)	-0.086 (3)	C(4)	-0.009 (3)
C(2)	-0.017 (3)	-0.081 (3)	C(5)	0.002 (3)
C(3)	0.012 (3)	-0.002 (3)	C(6)	-0.007 (2)
			C(7)	-0.011 (2)
			C(8)	-0.016 (2)
			C(9)	0.009 (2)
			C(10)	0.019 (3)
			C(11)	0.237 (3)

states at the Fermi surface. We get a total entropy change of  $\Delta S \approx 0.17 (2)R$ . Using the relationship  $\gamma T_c = \Delta S$  where  $\gamma = \pi^2 \rho(\epsilon_F) k_B^2$  and assuming a single band model, we can estimate  $\rho(\epsilon_F) \approx 5.7 \text{ eV}^{-1}$ . This is large compared to most metals since we have a quasi-one-dimensional system, and it is about twice as big as found for TTF-TCNQ. If two bands are assumed, these numbers would halve, but in any case, we have an increase in the density of states at the Fermi surface over TTF-TCNQ. Using the density of states from the above Fermi gas model and the ABB theory, we can estimate the size of the specific heat anomaly at the metal insulator transition. From the coefficients of a Landau free energy expansion,<sup>28,29</sup> we get  $\Delta C/R = 9.6 \rho(\epsilon_F) k_B T_c$  or  $\Delta C/R \approx 0.52$  which is in reasonable agreement with the experimental values.

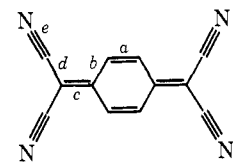
One way in which this change of density of states at the Fermi surface can be accomplished is by a change in the charge transfer between the donor and acceptor molecules, thereby altering the Fermi level within the band. One might expect that there would be differences in the degree of charge transfer at room temperature among the many derivatives of TTF-TCNQ. From the changes in the intramolecular bond lengths that are seen in TTF-DETCNQ when compared to TTF-TCNQ, we infer that the former compound has slightly less charge transfer than the parent system. On the basis of a simple tight bonding band model of a less than half-filled band, this would decrease the Fermi surface and increase the density of states which is important to the Peierls transition. However, it is unlikely that the charge transfer is the entire picture. The interplanar distances along the donor and acceptor chains increase by  $\sim 0.1 \text{ \AA}$  in going from TTF-TCNQ to TTF-DETCNQ. This should decrease the bandwidth,  $w$ , which also has the effect of increasing the density of states  $\rho(\epsilon_F)$  at the Fermi surface, in agreement with the specific heat measurements.

Knowing that we have an increase in the density of states at the Fermi surface, we examine the possible dependence of the transition temperature on this parameter. The tight binding model of a Peierls-Frohlich transition tells us that the transition temperature should go like  $k_B T_c = 2.28 w \exp(-1/\lambda)$  where  $w$  is the band width and  $\lambda$  is the electron phonon coupling parameter  $= 2\rho(\epsilon_F) g^2 / \hbar \omega(2k_F)$ ;  $\omega(2k_F)$  being the frequency of the phonon which gives rise to the Peierls distortion.

Table V. Bond Distances (Å) Averaged Over Assumed mmm Symmetry



	TTF-DETCNQ <sup>e</sup>	TTF-TCNQ <sup>a,e</sup>	TTF <sup>o</sup> b
$a$	1.367 (5)	1.372 (4)	1.349 (3)
$b$	1.750 (3)	1.745 (3)	1.757 (2)
$c$	1.720 (3)	1.739 (3)	1.726 (2)
$d$	1.323 (4)	1.326 (4)	1.314 (3)



	TTF-DETCNQ <sup>e</sup>	TTF-TCNQ <sup>a</sup>	TCNQ <sup>o</sup> c,e	TCNQ <sup>-1</sup> d
$a$	1.359 (3)	1.356 (3)	1.346 (3)	1.373 (4)
$b$	1.444 (3)	1.433 (3)	1.448 (4)	1.423 (4)
$c$	1.404 (3)	1.402 (3)	1.374 (3)	1.420 (4)
$d$	1.434 (3)	1.423 (3)	1.440 (4)	1.416 (4)
$e$	1.145 (3)	1.151 (4)	1.140 (3)	1.153 (4)

<sup>a</sup> Reference 7. <sup>b</sup> V. Schomaker and K. N. Trueblood, *Acta Crystallogr., Sect. B*, 24, 63 (1968). <sup>c</sup> R. E. Long, R. A. Sparks, and K. N. Trueblood, *Acta Crystallogr.*, 1, 932 (1965). <sup>d</sup> A. Hoekstra, T. Spoelder, and A. Vos, *Acta Crystallogr., Sect. B*, 28, 14 (1972). <sup>e</sup> Corrected for rigid-body motion. The TTF distances for TTF-TCNQ are only partially corrected (see A. J. Schultz, G. D. Stucky, R. H. Blessing, and P. Coppens, *J. Am. Chem. Soc.*, 98, 3194 (1976)).

If we include some interchain coupling which actually causes the transition to become ordered at a finite temperature this becomes<sup>35</sup>  $k_B T_c = (C/\lambda)^{1/4} 2.28 w e^{-1/\lambda}$ , where  $C$  is an interchain coupling parameter and  $C \ll \lambda$ . When  $\lambda$  is  $\leq 1$  as is true in TTF-TCNQ and we assume to be true in TTF-DETCNQ an increase in  $\lambda$  will cause an increase in the transition temperature since the exponential dominates both the effects of bandwidth in front of this expression and the effects of interchain coupling if we assume  $C$  to be fixed (or at least to be  $\ll \lambda$ ). We now examine how the changing value of the density of states might dominate the value of  $\lambda$ . First of all, changing the structure from system to system should effect the energy associated with the  $2k_F$  phonon but it is unlikely that this will change by a factor of two as we go from system to system with mass changes much less than a factor of two and small intrachain structural changes. What remains is  $\rho(\epsilon_F) g^2$ . In general these parameters cannot be decoupled. The tight binding model gives  $\rho(\epsilon_F)$  proportional to the inverse of a transfer integral  $t$ , and  $g^2$  proportional to  $t^2$  for acoustic phonon coupling so that  $\rho(\epsilon_F) g^2$  is proportional to the inverse of  $\rho(\epsilon_F)$  not to  $\rho(\epsilon_F)$  itself. This implies that an increase in the density of states would decrease the transition temperature, which we do not see. There are at least two cases where this is violated: when the change in density of states is caused by a change in charge transfer, not bandwidth, and when optical phonons are responsible for the electron phonon coupling. Both of these cases allow  $\rho(\epsilon_F)$  to vary without changing  $g^2$ , so that an increase in  $\rho(\epsilon_F)$  leads to an increase in  $\lambda$  and  $T_c$ . Although it is speculative to assert that this relationship between  $\rho(\epsilon_F)$  and  $\lambda$  holds for all materials similar to TTF-TCNQ, there is some evidence for this trend.

Kistenmacher et al.<sup>36</sup> have noted that methyl substitution on TTF should increase the charge transfer with TCNQ due to a decrease in the ionization potential of the TTF molecule. In those systems where substitution has been made on the TTF chain, the transition temperature has been observed to decrease.<sup>9,11,37</sup> This implies that the density of states at the Fermi surface is less in these systems than for TTF-TCNQ. Although

there are certainly many other variables involved, such as increased stacking distances, we might speculate that changes in charge transfer dominate changes in bandwidth for the substituted TTF compounds. For example, in (Me)<sub>4</sub>TTF-TCNQ, the increased interplanar distances are 3.53 and 3.26 Å for the cations and anions, respectively, but the transition temperature of 38 K<sup>37</sup> is lower than that for TTF-TCNQ.

If alkyl substitution on TTF increases its charge transfer with TCNQ because of a decrease in its ionization potential, substitution on TCNQ should have the opposite effect. That is, decreasing the ionization potential of TCNQ will make it more difficult to reduce TCNQ<sup>0</sup> to TCNQ<sup>x-</sup>, and therefore, the degree of charge transfer should decrease. Along with the longer repeat distance, this should result in a higher transition temperature, which we have observed for TTF-DETCNQ relative to TTF-TCNQ.

An additional observation about the conductivity should also be made. There is no peak in our conductivity measurements of TTF-DETCNQ. Moreover, despite the sharpness of the phase transition as shown in the specific heat measurements, the changes in the conductivity take place over a wide range in temperature. We believe that if there are conducting fluctuations associated with the Peierls-Frolich model in this system, they are masked by a large intrinsic property of the system, or by problems in crystal morphology.

**Acknowledgment.** The support of the National Science Foundation under Research Grant NSF DMR 7203026 is gratefully acknowledged.

**Supplementary Material Available:** Structure factors (10 pages). Ordering information is given on any current masthead page.

## References and Notes

- (1) (a) Department of Chemistry and Materials Research Laboratory; (b) Department of Physics and Materials Research Laboratory.
- (2) (a) J. Ferraris, D. O. Cowan, V. Walatka, and J. Perlstein, *J. Am. Chem. Soc.*, **95**, 948 (1973); (b) L. B. Coleman, N. J. Cohen, D. J. Sandman, F. G. Yamagishi, A. F. Garito, and A. J. Heeger, *Solid State Commun.*, **12**, 1125 (1973).
- (3) A. N. Bloch, R. B. Weisman, and C. M. Varma, *Phys. Rev. Lett.*, **28**, 753 (1972).
- (4) E. Ehrenfreund, S. Etemad, L. B. Collman, E. F. Rybaczewski, A. F. Garito, and A. J. Heeger, *Phys. Rev. Lett.*, **29**, 269 (1972).
- (5) P. N. Sen and C. M. Varma, *Solid State Commun.*, **15**, 1905 (1974).
- (6) S. Etemad, to be submitted for publication.
- (7) T. J. Kistenmacher, T. E. Phillips, and D. O. Cowan, *Acta Crystallogr., Sect. B*, **30**, 763 (1974).
- (8) A. N. Bloch, J. P. Ferraris, D. O. Cowan, and T. O. Poehler, *Solid State Commun.*, **13**, 753 (1973).
- (9) L. B. Coleman, M. J. Cohen, D. J. Sandman, F. G. Yamagishi, A. F. Garito, and A. J. Heeger, *Solid State Commun.*, **12**, 1125 (1973).
- (10) J. P. Ferraris, T. O. Poehler, A. N. Bloch, and D. O. Cowan, *Tetrahedron Lett.*, 2553 (1973).
- (11) R. Schumaker, M. Ebenhahn, G. Castro, and R. L. Greene, *Bull. Am. Phys. Soc.*, **20**, 495 (1975).
- (12) E. M. Engler and V. V. Patel, *J. Am. Chem. Soc.*, **96**, 7376 (1974).
- (13) K. Bechgaard, D. O. Cowan, and A. N. Bloch, *J. Chem. Soc., Chem. Commun.*, 939 (1974).
- (14) R. E. Pyle, A. N. Bloch, D. O. Cowan, K. Bechgaard, T. O. Poehler, T. J. Kistenmacher, V. V. Walatka, R. Banks, W. Krug, and T. E. Phillips, *Bull. Am. Phys. Soc.*, **20**, 415 (1975).
- (15) A. N. Bloch, D. O. Cowan, K. Bechgaard, T. O. Poehler, T. J. Kistenmacher, R. E. Pyle, R. Banks, and T. E. Phillips, *Bull. Am. Phys. Soc.*, **20**, 466 (1975).
- (16) G. R. Johnson, M. G. Miles, J. D. Wilson, and D. J. Dahm, *Bull. Am. Phys. Soc.*, **20**, 465 (1975); P. A. Berger, D. J. Dahm, G. R. Johnson, M. G. Miles, and J. D. Wilson, to be submitted for publication.
- (17) R. Groff, private communication.
- (18) R. C. Wheland and E. L. Martin, to be submitted for publication.
- (19) Some of the programs used in this work were local versions of Dewar's FAME program to calculate normalized structure factors, the Busing-Lévy ORFLS least-squares program, the Zalkin FORDP Fourier program, the Busing-Martin-Lévy ORFFE function and error program, and Johnson's ORTEP plotting program.
- (20) G. Germain, P. Main, and M. M. Woolfson, *Acta Crystallogr., Sect. A*, **27**, 368 (1971).
- (21) D. T. Cromer and J. T. Waber, *Acta Crystallogr.*, **18**, 104 (1965).
- (22) D. T. Cromer, *Acta Crystallogr.*, **18**, 17 (1965).
- (23) R. F. Stewart, E. R. Davidson, and W. T. Simpson, *J. Chem. Phys.*, **42**, 3175 (1965).
- (24) See paragraph at end of paper regarding supplementary material.
- (25) P. F. Sullivan and G. Seidel, *Phys. Rev.*, **173**, 679 (1968).
- (26) P. Handler, D. E. Mapother, and M. Rayl, *Phys. Rev. Lett.*, **19**, 356 (1967).
- (27) M. B. Salamon, *Phys. Rev. B*, **2**, 214 (1970).
- (28) R. A. Craven, M. B. Salamon, G. DePasquali, R. M. Herman, G. Stucky, and A. Schultz, *Phys. Rev. Lett.*, **32**, 769 (1974).
- (29) M. B. Salamon, J. W. Bray, G. DePasquali, R. A. Craven, G. Stucky, and A. Schultz, *Phys. Rev. B*, **11**, 619 (1975).
- (30) D. E. Schafer, G. A. Thomas, and F. Wudl, to be submitted for publication.
- (31) D. E. Schafer, F. Wudl, G. A. Thomas, J. P. Ferraris, and D. O. Cowan, *Solid State Commun.*, **14**, 347 (1974).
- (32) C. J. Fritchie, Jr., *Acta Crystallogr.*, **20**, 892 (1966).
- (33) V. Schomaker and K. N. Trueblood, *Acta Crystallogr., Sect. B*, **24**, 63 (1968).
- (34) D. Allender, J. W. Bray, and J. Bardeen, *Phys. Rev. B*, **9**, 119 (1974).
- (35) M. J. Rice and S. Strassler, *Solid State Commun.*, **13**, 125 (1973).
- (36) T. J. Kistenmacher, T. E. Phillips, D. O. Cowan, J. P. Ferraris, A. N. Bloch, and T. O. Poehler, to be submitted for publications.
- (37) T. J. Kistenmacher, private communication.